

Electron emission from carbon black-based field emitters including diesel engine exhaust

H. Busta,^{a)} D. Boldridge, R. Myers, and G. Snider
Cabot Microelectronics Corporation, Aurora, Illinois 60504

A. Korotkov
University of California, Riverside, California 92521

E. Edwards and A. Feinerman
University of Illinois, Chicago, Illinois 60607

(Received 6 October 2003; accepted 12 January 2004; published 1 June 2004)

Field emission properties of carbon black, carbon black and silica, and diesel engine exhaust were investigated and compared to multiwall carbon nanotubes prepared in a similar manner. Sample preparation consisted of pressing the nanopowders into pellet form, dispersing them in isopropanol, or dispersing them in Shipley S1818 photoresist to achieve better adhesion to the substrates. Turn-on fields, at room temperature, ranged from 3–6 V/ μm for the pressed and isopropanol prepared samples and shifted to 10–18 V/ μm for the photoresist dispersed samples. At 120 °C, the turn-on fields for the photoresist dispersed samples shifted to lower values. This very strong temperature dependence is explained by a resonant Fowler–Nordheim tunneling model. It assumes that a thin barrier layer forms at the elevated temperatures due to outgassing/sublimation events. The macroscopic current densities reached for these samples are about 1–2 mA/cm². © 2004 American Vacuum Society. [DOI: 10.1116/1.1667517]

I. INTRODUCTION

The field of vacuum microelectronics is undergoing quite an evolution since the first International Conference was held in Williamsburg, VA in 1988. During the 1990's, emphasis was placed on the fabrication of gated molybdenum cone devices—the Spindt emitter. Each cone was surrounded by its own micromachined gate and several hundred to thousand gated cones constituted one pixel element in a field emitter display (FED). With the realization that tiny carbon nanotubes (CNTs) form excellent field emitters,¹ a pixel element now consists of CNTs dispersed in a paste that is applied to a substrate by thick-film screening methods. Thus, well controlled and expensive large area thin-film fabrication is replaced by lower cost thick-film technology. The array of gates per Spindt tip is replaced by an array with much larger gate openings. In some cases, there is only one gate opening per pixel element. These gates can be of the top version² or of the undergate-type version.³ One important element in achieving the desired pixel uniformity is by an activation process either by laser² or plasma treatment.⁴ These processes release some of the nanotubes from the paste, creating a fuzzlike appearance on the top surface of the pixel elements. Thirty-eight in. diagonal FED prototypes have been fabricated using the CNT paste technology.³ Another reason for replacing molybdenum emitters with CNTs is the fact that CNTs exhibit a higher resistance toward sputter-induced events.

At present, CNTs are expensive to produce and have to go through an expensive and time consuming grinding and milling process before they can be printed onto a substrate. In

this article, an alternative source material, carbon black, is investigated for its suitability as a field emitter. It is extremely low cost and produced in large quantities. The main applications are as a feedstock for tires and inks. In addition to carbon black, carbon black mixed with silica—also a very inexpensive feedstock for chemical mechanical planarization slurries—is investigated. The idea was to form nanosize triple junctions where conductor, insulator, and vacuum meet. At the interface of a triple junction, enhanced field emission can take place.⁵ Diesel engine exhaust, which is a contaminated form of carbon black and also available in abundance, is also investigated. The performance of all three types of field emitters is compared to the performance of CNTs.

II. SAMPLE PREPARATION

Carbon black, Vulcan-XC72R, GP3820, and silica, Cab-O-Sil, L-90, lot 1L165, were purchased from Cabot Corporation, Boston, MA. The diesel engine exhaust was collected at the end of the exhaust pipe of a Gordon Food Services, Grand Rapids, MI, four-cylinder Sterling diesel engine, serial No. 5217. The carbon nanotubes were supplied by Dr. Wei Zhu of Bell Laboratories and Lucent Technologies. Initial samples were prepared by pressing the powder into pellets using a screw-type press. The pellets of carbon black and carbon black/silica (equal amounts by weight) were then attached to a copper-coated silicon substrate using silver paint. Turn-on fields of about 3–6 V/ μm were obtained, but adhesion to the substrate and of the particles to each other were poor and resulted in pull outs as the electric field was increased. Some samples were also prepared by dispersing carbon black and carbon black/silica (equal amounts by weight)

^{a)}Electronic mail: heinz_busta@cabotcmp.com

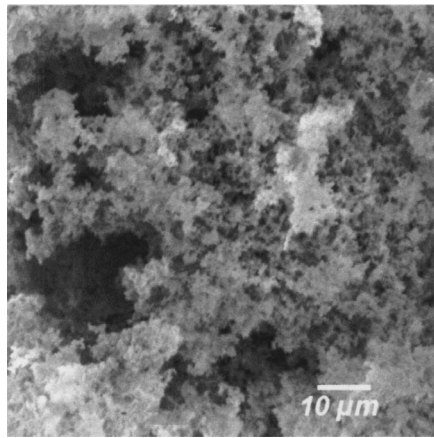


FIG. 1. SEM image of the top view of carbon black and silica dispersed in isopropanol after the isopropanol evaporated.

in isopropanol. Several drops of these mixtures were deposited onto a copper-coated silicon wafer and spun at about 300 rpm. Turn-on fields were also in the 3–5 V/ μm range and adhesion was also poor.

To improve adhesion, the powders were then dispersed in Shipley S1818 positive photoresist and spun onto copper-coated silicon substrates at 5000 rpm. The samples were then baked in air at 120 °C for about 5 min. In most cases, about equal amounts, in volume, of the powders and photoresist were used. The powders were mixed into the photoresist with a spatula or glass rod and then ultrasonically agitated for 5–10 min. Representative scanning electron microscope (SEM) images of some of the samples are shown in Figs. 1–4. Additional SEM images are presented in Refs. 6 and 7. Figure 1 shows the SEM image of the top view of carbon black and silica dispersed in isopropanol. Figure 2 shows the cross section of carbon black and silica dispersed in Shipley S1818 photoresist after spinning and baking on a copper-coated silicon wafer. The average film thickness is about 3 μm with a surface roughness of $\pm 1.5 \mu\text{m}$. The top view of a sample of carbon black and silica dispersed in S1818 is

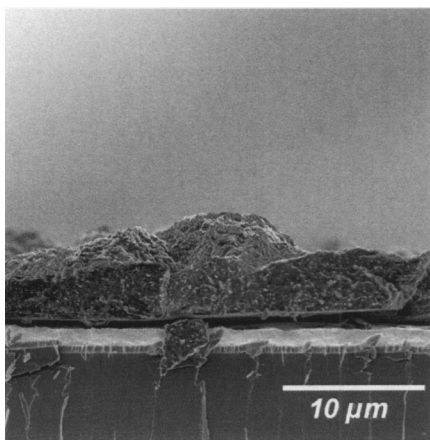


FIG. 2. SEM image of the cross section of carbon black and silica dispersed in Shipley S1818 photoresist. The film is deposited onto a copper-coated silicon substrate and baked in air at 120 °C.

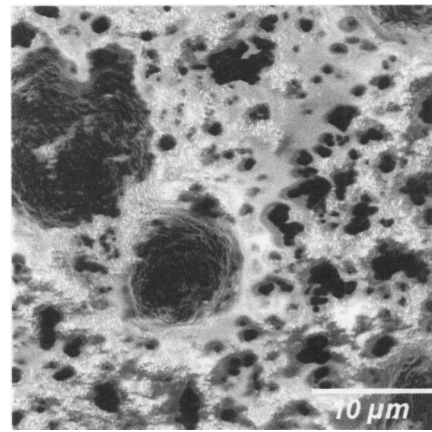


FIG. 3. SEM image of the top view of carbon black and silica dispersed in Shipley S1818 photoresist after baking in air at 120 °C. Carbon/silica islands form between photoresist islands. The packing density depends on the volume fraction of the carbon black/silica powders.

shown in Fig. 3. One can observe segregation of the carbon black/silica powder into different size islands separated by regions of photoresist. Depending on the amount of powder and the addition of suitable dispersants, a more uniform distribution of the powders within the photoresist can be obtained. Figure 4 shows the SEM image of untreated diesel engine exhaust dispersed in S1818 photoresist. For this sample, the film was not spun onto the wafer but was deposited using a spatula.

III. EXPERIMENTAL RESULTS

A. Vertical resistance

In order for the films to be able to emit electrons, it is necessary for them to be conductive, at least in the vertical direction. Electrons have to be transferred from the substrate, through the film, to the film/vacuum interface. To measure vertical conduction, a tungsten probe, shaped into a loop was brought into contact with the film surface, with the plane of the loop positioned parallel to the film surface. This procedure prevents accidental piercing of the film with the sharp probe tip. Current–voltage (I – V) curves through the film

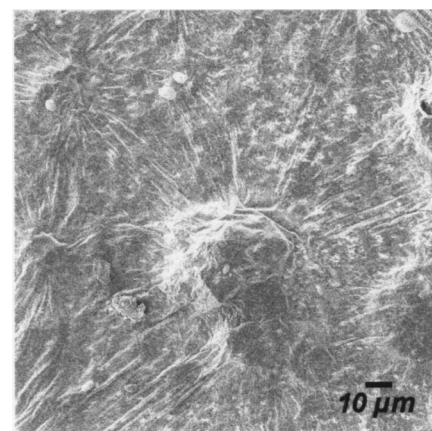


FIG. 4. SEM image of untreated diesel exhaust dispersed in Shipley S1818 photoresist after baking in air at 120 °C.

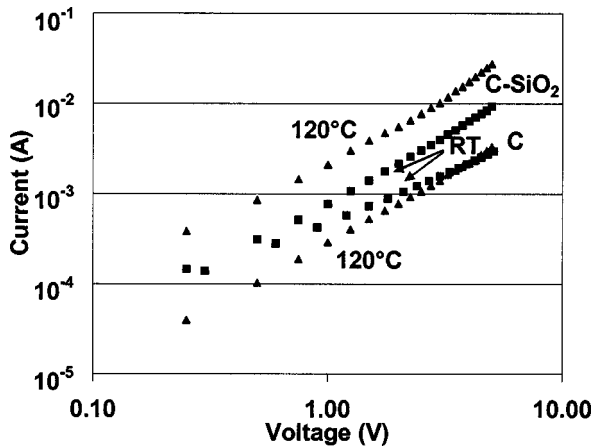


FIG. 5. I - V curves of carbon black/photoresist and carbon black/silica/photoresist samples in the vertical direction. The measurements were performed at RT and at 120 °C.

were obtained with an Agilent Parameter Analyzer, Model 4155C. Figure 5 shows the I - V curves of carbon black/photoresist and carbon black/silica/photoresist at room temperature (RT) and at 120 °C. Similar data were taken for diesel engine exhaust/photoresist and carbon nanotubes/photoresist.⁷ The currents through the films are in the mA range at voltages below 10 V. This is more than adequate since the maximum emission currents obtained from these samples are only 0.1–0.2 mA. The temperature dependence is reversed for the two samples. This fact, by itself, is of some interest (metallic versus semiconductive behavior) but is of no consequence for the results presented below.

B. Emission results

Emission testing was performed in an ion-pumped vacuum system at pressures ranging from 5×10^{-9} to 1×10^{-7} Torr. The extraction electrode consists of a 3 mm diameter, flat polished tungsten probe that was positioned from 50–125 μm from the film surface. The probe is mounted on an XYZ manipulator. Figure 6 shows the emission current–extraction field (I - E_0) curves for several films

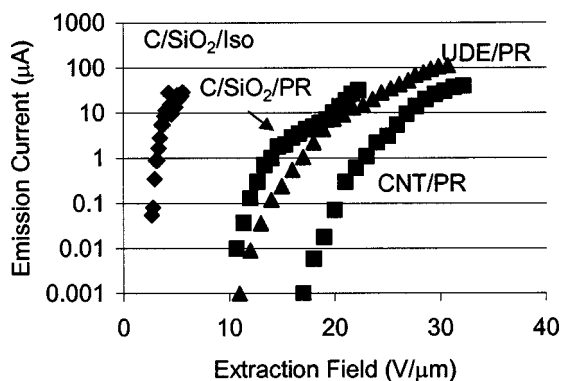


FIG. 6. I - E_0 results for carbon black/silica/isopropanol, carbon black/silica/photoresist, untreated diesel exhaust/photoresist, and carbon nanotubes/photoresist samples measured at room temperature.

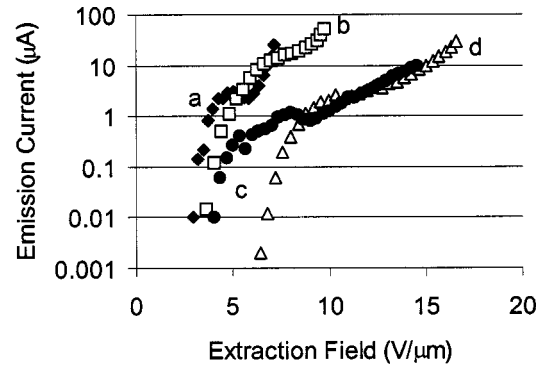


FIG. 7. I - E_0 results for (a) carbon black/silica/photoresist, (b) carbon nanotubes/photoresist, (c) untreated diesel exhaust/photoresist, and (d) carbon black/photoresist samples measured at 120 °C.

measured at RT. The extraction field E_0 is defined as the probe voltage divided by the electrode-to-film surface distance. From these results, one can see that the C/SiO₂/isopropanol sample has the lowest turn-on field. The turn-on field is defined as the field when the current reaches about 10 nA. When the powders are dispersed in photoresist, the turn-on fields shift to larger values. The I - E_0 curves shown in Fig. 6 represent measurements after the films have been conditioned. Since it is very likely that a thin photoresist layer is on top of the carbon particles or nanotubes, this thin layer has to be either removed or made conductive. This is accomplished by repeatedly measuring the I - E_0 curves until they become reproducible. The E_0 values for the first run are in most cases higher than the data indicate in Fig. 6. Similar conditioning had to be performed for Pd nanoparticles dispersed in photoresist⁸ and for Si tip emitters to generate a sufficient number of defect states in the native oxide to render it conductive or to electrodesorb it. From Fig. 6, it could be concluded that the CNT/photoresist sample is the poorest performer. However, these results depend very strongly on the volume fraction of the powders, the deposition conditions, and also the region on the substrate where the data are being taken. Also, no significant difference was observed between the C/photoresist and the C/SiO₂/photoresist samples. It cannot be concluded that the inclusion of SiO₂ into the samples yields improved results, i.e., lower turn-on fields, due to a triple junction effect.

Figure 7 shows the emission results at 120 °C for the same group of samples shown in Fig. 6, except for the isopropanol dispersed sample. The turn-on fields moved to lower values and the shape of the I - E_0 curves changed.

IV. RESONANT FOWLER–NORDHEIM TUNNELING MODEL

The shape of all four curves in Fig. 7 consists of an initial steep rise in current with field, followed by a lower slope region or even a maximum/minimum, followed again by a steep rise. This type of general I - E behavior has been observed for other emitters as well and is attributed to different effects. For laser ablated BN and polycrystalline diamond films, the initial rise was interpreted as Fowler–Nordheim

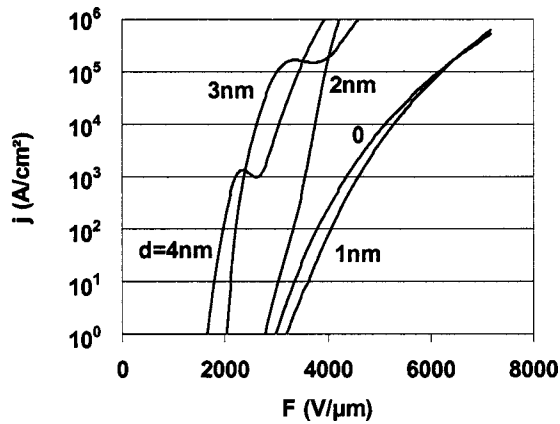


FIG. 8. Theoretical j - F curves for barrier layer thicknesses of 0, 1, 2, 3, and 4 nm using the rF-N tunneling model (presented in Ref. 11).

(F-N) tunneling, followed by a shallow region caused by a large film resistance, followed by a steeper rise in which the film resistance decreased significantly as a function of field (bias). Measurements of the voltage dependent film resistance were correlated to the I - E curve.⁹ For the solid-state emitter, which consists of a 5 nm thick titanium oxide layer on top of platinum, the steep initial rise is attributed to F-N tunneling, followed by a thermionic event, followed by an “explosive” event.¹⁰ For CNTs, it is suggested that the initial sharp rise is caused by resonant tunneling enhanced emission from adsorbates, followed by desorption (the flat region), followed by F-N emission from the clean surface.¹ If that was indeed the case, then by reversing the field, a different I - E_0 trace should be obtained. This is not the case for the emitters presented here, as has been shown for the C/SiO₂/photoresist sample in Fig. 7.⁶ Within experimental noise of the measurements, the I - E_0 trace is identical for increasing and decreasing fields.

To explain the data, at least semiquantitatively, in Figs. 6 and 7 (except for the isopropanol data), the resonant F-N (rF-N) tunneling formalism developed in Ref. 11 has been adapted. It is assumed that a thin barrier layer of adsorbates exists on top of the film and that its thickness increases as a function of temperature due to outgassing and/or sublimation events. By applying a bias to the extraction electrode, the energy barriers take on a triangular shape and quantum states appear in the well between the barrier film and the vacuum level.^{7,11} By changing the field, the quantum states move with respect to the Fermi level, causing a resonance effect as they align. The shape of the I - E curves depends strongly on the thickness of the barrier layer. Figure 8 shows the model calculations, current density j versus vacuum field F (j - F) for barrier widths of $d=0, 1, 2, 3,$ and 4 nm. The parameters used in these calculations are: Work function $\Phi=4.2$ eV, barrier height $U=0.8$ eV, dielectric constant of the barrier film $\epsilon=4.5$, and effective masses in the substrate and barrier $m_s=0.2m_e$, $m_b=0.42m_e$, with m_e as the free electron mass. The j - F curves, which are calculated for planar films, depend very strongly on the thickness of the barrier film. Similar to the experimental data shown in Figs. 6 and 7, the

curves move toward lower-field values as the barrier thickness increases and peaks, similar to the ones in Fig. 7, appear. In Ref. 7, it is demonstrated for the diesel engine exhaust data how the theoretical curves in Fig. 8 can be used to fit the data. From the RT data, where it is assumed that the thickness of the barrier height is below 1 nm, the F-N parameters for the field enhancement factor β and the emission area α are obtained. These values are then used to convert the calculated j - F curves into the experimental I - E_0 curves by using the relationships $I=\alpha j$ and $E_0=F/\beta$. Reasonable agreement between experiment and theory is obtained and similar calculations can be performed for the other samples. Additional work has to be performed to establish that, indeed, such a barrier layer exists and that its thickness increases with temperature. Also, by obtaining its dielectric constant and barrier height, the model calculations can be improved.

V. SUMMARY

It was demonstrated that carbon black and carbon black/silica, in pellet form or dispersed in isopropanol, function as reasonably good field emitters with turn-on fields ranging from 3–6 V/ μ m. The adhesion to the substrate was poor and portions of the films were pulled from the substrate at elevated fields. To improve adhesion, carbon black and carbon black/silica were dispersed in Shipley S1818 positive photoresist. Adhesion was excellent, but turn-on fields, at RT, increased to about 10–18 V/ μ m. Macroscopic current densities (maximum emission current divided by the area of the extraction electrode) of 1–2 mA/cm² were reached. This compares very well with quoted current densities for carbon nanotubes mixed in printable pastes.² A strong temperature dependency of the emission currents was observed at 120 °C resulting in a shift of the turn-on fields to lower values and in the formation of peaks in the I - E_0 curves. A big surprise occurred when carbon black was substituted with untreated diesel engine exhaust. Similar emission behavior is obtained. The emission data were compared to samples in which carbon black was substituted with multiwall CNTs. Similar behavior is obtained with no significant advantage being offered by the CNTs. The above samples serve as a model case study of rF-N tunneling through an adsorbate film whose thickness changes with temperature due to outgassing/sublimation events. No recourse has to be made to changing film resistance, explosive events, or desorption phenomena, as is necessary in previously proposed models. No systematic difference in emission behavior between the carbon black and carbon black/silica samples was observed. Thus, carbon black, a very inexpensive material, has the potential to replace expensive CNTs as a source material in field emitter pastes.

ACKNOWLEDGMENTS

The authors would like to thank S. Steckenrider, C. Hawes, A. Kalesinskiene, R. Sevilla, B. Zwicker, and J. Jones of Cabot Microelectronics Corporation for their contributions to this work, and Professor K. Likharev of State

University of New York at Stony Brook for supplying us with the rF–N computer model and the interpretation of the results. Thanks also go to R. Lajos and E. Elzy of UIC for keeping the high-vacuum system in excellent operating condition.

¹*Vacuum Microelectronics*, edited by W. Zhu (Wiley, New York, 2001), Chap. 6

²K. Nishimura *et al.*, *Technical Digest of the 16th International Vacuum Microelectronics Conference*, Osaka, Japan (2003), O5-4.

³C. G. Lee *et al.*, *Technical Digest of the 16th International Vacuum Microelectronics Conference*, Osaka, Japan (2003), I5-1.

⁴Y. Kanazawa, T. Oyama, K. Murakami, and M. Takai, *Technical Digest of the 16th International Vacuum Microelectronics Conference*, Osaka, Japan (2003), P2-33.

⁵R. V. Latham, *High Voltage Vacuum Insulation: The Physical Basis* (Academic, New York, 1981), p. 229.

⁶H. Busta, D. Boldridge, R. Myers, E. Edwards, and A. Feinerman, *Appl. Phys. Lett.* **83**, 1779 (2003).

⁷H. H. Busta, R. E. Myers, A. N. Korotkov, E. H. Edwards, and A. D. Feinerman (unpublished).

⁸A. Baba and T. Asano, *J. Vac. Sci. Technol. B* **21**, 552 (2003).

⁹H. Busta and R. Pryor, *J. Appl. Phys.* **82**, 5148 (1997).

¹⁰V. T. Binh and C. Adessi, *Phys. Rev. Lett.* **85**, 864 (2000).

¹¹A. N. Korotkov and K. K. Likharev, *Appl. Phys. Lett.* **75**, 2491 (1999).